TRR
JOURNAL OF THE TRANSPORTATION RESEARCH BOARD

Article

Transportation Research Record
2018, Vol. 2672(8) 199–209

DOI: 10.1177/0361198118793519
journals.sagepub.com/home/trr
SAGE

Evaluation of Route Changes Utilizing High-Resolution GPS Bus Transit Data

Travis B. Glick[1] and Miguel A. Figliozzi[1]

Abstract

This study applies high-resolution archived transit data to study the effect of roadway changes using data collected before and after the completion of a project affecting transit. Methodologies are presented to compare percentile and time-of-day performance measures before and after the project. In addition, differences in travel time and travel-time variability are examined over the altered route. The case study examines one heavily used route in Portland that was recently diverted onto a newly built transit-only bridge to examine the claims that travel times would decrease and reliability would increase. The results of this study indicate that travel times increased for the majority of trips but travel-time variability during the peak period was sharply reduced.

Methodologies to quantify transit performance influence transportation planning and subsequent decisions; those decisions may affect operating speeds, travel times, ridership, costs, and efficiency (*1*). Transit operations research is continually evolving with the introduction of new or improved data-collection systems. Onboard global position systems (GPS) are opening up new research opportunities to visualize and quantify transit behaviors hidden by legacy data-collection systems. High-resolution (HR) GPS data-collection is expanding analysis options when implemented. However, these data-collection systems are new, not widespread, and as a result, understudied.

This study applies HR data to quantify the impact of changes to roadways as a before-and-after study. This study expands on existing systems to show applicable methodologies that quantify transit performance changes following a roadway modification in locations where transit has been traditionally excluded.

The case study for this paper examines the effect of the Tilikum Crossing. This new bridge in Portland, OR is the largest vehicle-free bridge in the United States (*2*). Although it is designed for light rail, streetcar, bikes, buses, and pedestrians, personal vehicles are not permitted. TriMet, Portland's public transportation provider, claimed the new bridge would reduce travel times and improve efficiency on routes 9 and 17 (*3*). This paper examines those claims for Route 9. The bridge cost was estimated at US$134 million paid for by federal grants, OR state lottery, and TriMet revenue.

Background and Literature Review

Before-and-after studies are not new, and frequently seek to quantify effects of roadway modifications. These studies exist across transportation modes and roadway applications. Their widespread implementation is one of the main ways new systems are adopted.

These studies typically use Bayesian statistics or are descriptive in nature. Studies that use Bayesian methodologies for before-and-after analysis reach back more than 30 years. The literature on Bayesian methodologies up to 2006 is well summarized in a paper that claims that a lack of sufficient data, such as traffic or crash counts, leads to high levels of uncertainty (*4*). Due to the natural variation in count data, crash rates fluctuate wildly month-to-month and year-to-year. Improvements for count usage have been proposed by newer papers that have added observations to reduce uncertainty by including additional counts estimated from models, which are based on locations with physical similarities to a given study area. These counts are then modified using a known prior distribution (*5*, *6*).

[1]Transportation Technology and People Lab, Department of Civil and Environmental Engineering, Maseeh College of Engineering and Computer Science, Portland State University, Portland, OR

Corresponding Author:
Address correspondence to Miguel A. Figliozzi: figliozzi@pdx.edu

Traffic assessment often uses descriptive before-and-after approaches. For example, a study looking at the change in fatal crashes following the introduction of anti-lock brakes compared results using the difference in an estimated risk ratio and its associated 95% confidence interval (CI) calculated from the collected data (*7*). Researchers have also examined the effect of traffic-calming systems across the United States for pedestrian wait times, using *t*-tests to measure differences in mean values (*8*). Descriptive analyses are appropriate for large sample sizes and appear across many fields.

This study did not use counts, which therefore limited the application of Bayesian methodologies. Variance of speed data was calculated using asymptotic variance and a probability mass function (9) described in the methodology section of this paper. Additionally, this research employed recently published performance metrics methodologies that use percentile travel-time, travel speed, and CI estimates to identify and rank low-performance hotspots (*10*). Percentiles are more general and suited for both symmetric and skewed distributions; for example, off-peak travel follows lognormal distributions, which are asymmetric.

Travel times play a key role in the overall ridership of a city. Travel-time elasticity is not readily available for all cities, as noted by Ayvalik et al. for Chicago (*11*); however, Portland, OR is a city with a full travel-forecasting model (*12*). This model indicates that decreased transit travel-times will increase overall ridership. When estimating travel times and trajectories, researchers have used proxies. Early research using buses as probes showed that buses experience the same types of delays as automobiles but that the reverse relationship is not always true. For example, buses will dwell at designated locations (bus stops) that regular vehicles do not (*13*, *14*). TriMet buses have been used widely to quantify arterial performance for both automobiles and transit (*15*, *16*).

Stop event (SE) data collects information at each bus stop including, but not limited to, actual and scheduled times of arrival and departure, dwell times, door usage, and passenger movements. When combined with data from loop detectors, signal cycle lengths, and other proprietary data-collection systems, SE data has been used to estimate travel times of other factors that may influence service reliability at the point, stop-to-stop, and route levels (*13, 17–19*). Each new study adds useful information, but the representation remains an average between stops due to the nature of SE data. Stop disturbance (SD) data, which includes information about any location where the wheels of the bus have stopped, such as the type (i.e., scheduled or unscheduled), location, and time of stop, may be combined with SE data to provide insights into stopping behavior associated with intersections or locations with heavy congestion. The integration of HR data with SE data may be used to mitigate some of the shortcomings of SE or SD data. For example, one study using GPS data found that for narrow ranges of departure times, travel-time distributions are best characterized by normal distributions. The same is true for peak-hour travel windows, but off-peak travel-times follow lognormal distributions (*20*).

Data Sources

This study relied on data provided by the Tri-County Metropolitan Transportation District of Oregon (TriMet), which has archived automatic vehicle location (AVL) data for all trips since 1997. TriMet updated their bus dispatch system with HR data collection in 2013. SE, SD, and HR data are the foundation of TriMet's collection systems. TriMet also creates onboard video recordings of all trips; however, TriMet, as with many agencies, erases video on a weekly cycle unless an incident occurs or if requested for a specific date (*21*).

At the authors' request, TriMet provided three sets of AVL data: SE, SD, and HR. Each of the AVL data sets represent the same buses, routes, and times; this allows for comparisons and integration of the data sets. The visuals and comparisons obtained using a combined data set provide additional details, hidden or not included in each of the sets individually.

For the before case, there were 1,227 and 1,158 buses in the eastbound and westbound directions, respectively. The after case had 1,453 and 1,691 buses in the eastbound and westbound cases, respectively.

Study Areas

The changes to bus operations on Southeast Powell Boulevard (Powell) resulted from the completion of the Tilikum Crossing, a new bridge over the Willamette River. This bridge was built to carry light rail, streetcars, and buses. Route 9, which historically crossed the Ross Island Bridge, was diverted to the new crossing. The changes examined are for the section where the two different routes converge on the east side of the river. In addition to the travel speed percentile comparisons, Powell was also examined statistically for changes by time of day to isolate when the roadway saw increases in speed.

Typically, this area of Powell is highly congested and carries upwards of 40,000 vehicles daily. However, no traffic counts are available for this stretch of Powell from 2016. Data collected at the macroscopic level (i.e., Portland region), mostly on freeways, indicate the peak periods are lasting longer across the metro area and that daily vehicle miles traveled, daily congestion hours, and daily vehicle hours of delay increased by

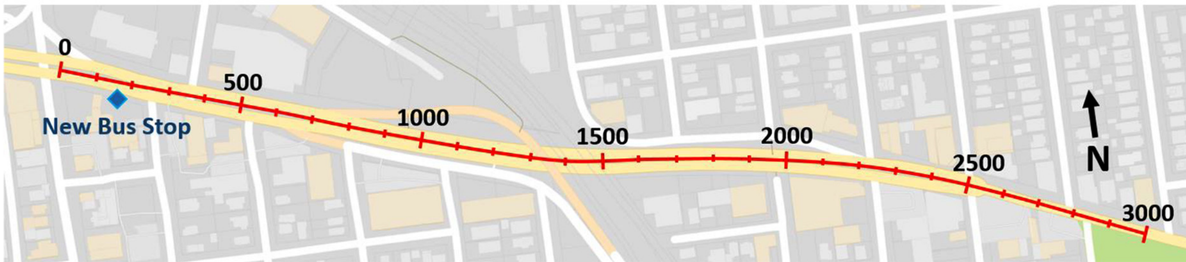

Figure 1. Map of study area for Southeast Powell Boulevard. Measurements correspond to x-axis of results.

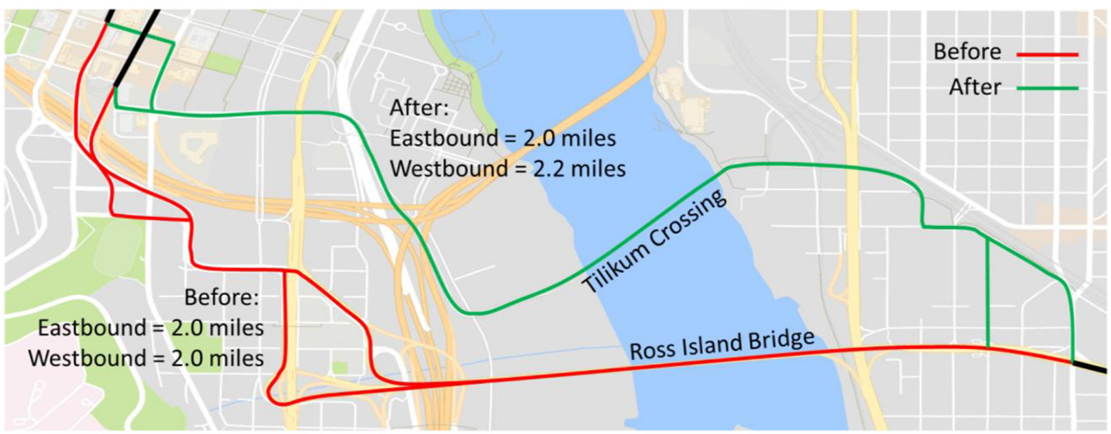

Figure 2. Map of route before and after change. Red shows the previous configuration. Green shows the new configuration.

approximately 1%, 11%, and 17%, respectively from 2014 to 2016 (*22*).

Figure 1 shows the study area leading up to the changed route on the east side of the river. This segment saw no physical changes but is examined for performance changes that may be the result of the new route.

Figure 2 shows the change in route. The distance traveled by eastbound buses was unchanged. Westbound buses now travel an additional 0.2 miles (~322 meters).

Methodology

The three data sets provided by TriMet cover the same time period, routes, and buses, with some exceptions caused by different data-collection parameters. These data sets must be filtered and cleaned to provide a uniform set of trips, which requires a unique identification number across the sets. All data sets include a bus number, trip number, and date; these serve as a starting point. Individual trips are separated based on route and direction included in the SE and SD data sets. The HR data, which does not include these identifiers, must be compared with the other sets to separate out individual trips based on time. This process culminates in a unique identification number for each bus and trip across all the data.

Using the unique identification number, all three data sets are integrated starting with the SE and SD data sets. When a bus dwells at a bus stop, these locations are considered SDs, so these events are duplicated, whereas pass-by stops would not be recorded. The integration of the data sets ensures that pass-by stops, dwell events, and other places where the wheels of the bus stop moving are all included with as much detail as can be provided by the combination of both sets.

Following this step, the HR data is interwoven by timestamps with the SE and SD data to provide a complete picture of the bus's trajectory, an example of this is shown in Figure 3. The merged data sets provide a means to quantify roadway behaviors that account for and can exclude bus-stopping behavior, which allows for estimates of general traffic behavior.

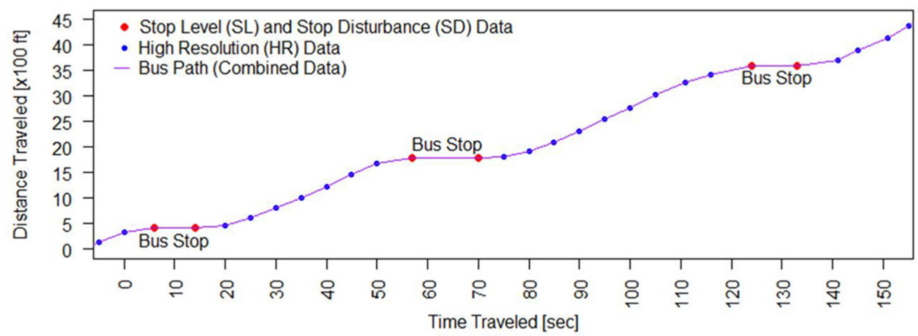

Figure 3. Bus trajectory using the combined data set.

Each study area is divided into a system of equal length and non-overlapping segments, s_i. Each unique segment shall be given an index of i. The total number of segments shall be denoted as n_I.

$$i \in I = \{1, 2, 3, \ldots, n_I\}$$

The combined data will have a set of j bus trip that pass through each segment, s_i. The consecutive GPS coordinates that surround each centerpoint of a given segment, s_i, are extracted to make up a pair of GPS coordinates (or vehicle trips) for each s_i. The total number of vehicle trips in each segment is denoted as n_{J_i}.

$$j \in J_i = \{1, 2, 3, \ldots, n_{J_i}\}$$

The data used in the analysis deviates from normal distributions. As such, this study relies heavily on percentiles and their associated percentile variances. The methodology for calculating speeds stems from a previously published paper using HR data (*10*), but with a procedure that allows the estimation of CIs when distributions are not necessarily normal. Any s_i has a set of percentile travel speeds found by ordering the data and extracting a number that correspond to a percentile, p. The value of the speed percentile in segment$i$ is denoted $v_{i,p}$. The standard deviation of the estimated $v_{i,p}$ is denoted $\sigma_{i,p}$.

The process to estimate each $\sigma_{i,p}$ is described in Figure 4. For example, Figure 4 upper left shows the speed histogram for any segment i. A cumulative distribution function (CDF) is estimated from the data (upper right) and later spline smoothing is applied to the CDF to create a continuous function that approximates the CDF (lower left). From this generated spline-smoothed function, the probability of a given point can be calculated by taking the derivative of the CDF to produce an estimate of the probability density function (PDF) – see lower right. This process can be applied to any probability distribution.

The estimate of the variance for any percentiles of univariate data is estimated through a CDF and its derivative, the PDF. To estimate $\hat{\sigma}_{v_{i,p}}{}^2$, the variance of a speed percentile, the following equation is utilized (*23*):

$$\hat{\sigma}^2_{v_{i,p}} = \frac{p(1-p)}{f\left(\hat{v}_{i,p}\right)^2 \cdot n_{J_i}}$$

where $f\left(\hat{v}_{i,p}\right)$ is the probability of the PDF given the input velocity, $\hat{v}_{i,p}$, and n_{J_i} is the number of observations in each segment i. Assuming the number of observations is large ($>$160) (*23*), this estimate of variance may be used to estimate the CIs for each $\hat{v}_{i,p}$. For a confidence level α and its associated z-score, $z(\alpha)$, the range of percentile values that may represent an estimated percentile is found.

$$CI_{\hat{v}_{i,p}} = \left[\hat{v}_{i,p} - \hat{\sigma}_{v_{i,p}} \cdot z(\alpha), \hat{v}_{i,p} + \hat{\sigma}_{v_{i,p}} \cdot z(\alpha)\right]$$

This interval provides the indices for the extremes of the CI around $v_{i,p}$.

A speed variability $\Delta\hat{v}_i$, is used to identify segments that are more heavily congested during the peak hour (*21*). It is calculated by subtracting the 15th percentile travel speed from the 85th percentile travel speed. When divided by the median travel-time, a speed variability index $(\hat{\mu}_i)$ is obtained for each segment (*21*).

$$\Delta\hat{v}_i = \hat{v}_{i,85} - \hat{v}_{i,15}$$

$$\hat{\mu}_i = \frac{\Delta\hat{v}_i}{\hat{v}_{i,50}} = \frac{\hat{v}_{i,85} - \hat{v}_{i,15}}{\hat{v}_{i,50}}$$

The standard deviation of the estimated Δv_i can be estimated as follows:

$$\hat{\sigma}_{\Delta v_i} = \sqrt{\hat{\sigma}^2_{v_{i,85}} + \hat{\sigma}^2_{v_{i,15}} - 2 \cdot cov(\hat{v}_{i,85}, \hat{v}_{i,15})}$$

Note that this formula for $\hat{\sigma}_{\Delta v_i}$does not require that the distributions be normal for large enough sample sizes.

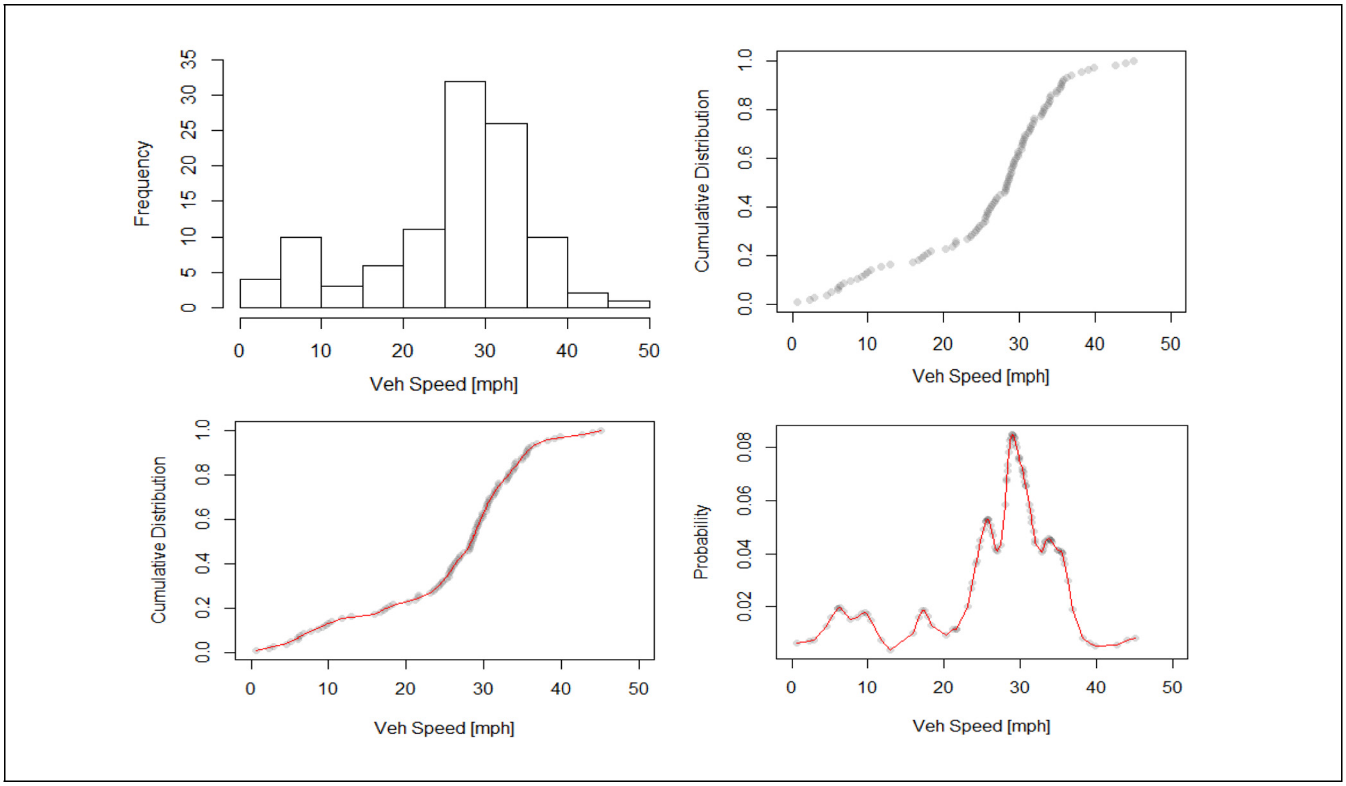

Figure 4. Upper left: histogram of randomly generated data in 5-mph (~8-kph) bins. Upper right: actual cumulative distribution of points. Lower left: cumulative distribution function creating through spline smoothing. Lower right: probability mass function for data.

As the speed percentiles are not independent, the covariance increases the estimation CI:

$$CI_{\Delta v_i} = [\Delta\hat{v}_i - \sigma_{\Delta\hat{v}_i} \cdot z(\alpha), \Delta\hat{v}_i + \sigma_{\Delta\hat{v}_i} \cdot z(\alpha)]$$

If 0 falls within the estimated interval, the null hypothesis $\Delta\hat{v}_i = 0$ cannot be rejected using a confidence level based on α.

The standard deviation of the estimated μ_i can be approximated as follows utilizing a well-known formula for propagation of uncertainties (*24*) assuming uncorrelated speed percentiles:

$$\frac{\hat{\sigma}_{\mu_i}}{|\hat{\mu}_i|} \sim \sqrt{\left(\frac{\hat{\sigma}_{\Delta v_i}}{\Delta\hat{v}_i}\right)^2 + \left(\frac{\hat{\sigma}_{v_{i,50}}}{\hat{v}_{i,50}}\right)^2} =$$

$$\sqrt{\frac{\hat{\sigma}_{v_{i,85}}{}^2 + \hat{\sigma}_{v_{i,15}}{}^2 - 2 \cdot cov(\hat{v}_{i,85}, \hat{v}_{i,15})}{\hat{v}_{i,85} - \hat{v}_{i,15}{}^2} + \left(\frac{\hat{\sigma}_{v_{i,50}}}{\hat{v}_{i,50}}\right)^2 + \left(\frac{\hat{\sigma}_{v_{i,50}}}{\hat{v}_{i,50}}\right)^2}$$

As the speed percentiles are not independent, the estimated σ_{μ_i} using the previous equation is a lower bound. The value $\hat{\sigma}_{\mu_i}$ can be used to estimate a lower bound CI for $\hat{\mu}_i$:

$$CI_{\mu_i} = \left[\hat{\mu}_i - \sigma_{\hat{\mu}_i} \cdot z(\alpha), \hat{\mu}_i + \sigma_{\hat{\mu}_i} \cdot z(\alpha)\right]$$

If 0 falls within the estimated interval, the null hypothesis $\hat{\mu}_i = 0$ cannot be rejected using a confidence level based on α.

The methodologies described provide the foundation to compare the initial and changed conditions of the study area. For all the data, before-and-after data will be designated by sub-indexes 0 and 1, respectively. A δ added before a variable will denote the difference between after and initial conditions. The differences in the means and percentile speeds and travel times and peak-hour performance metrics are denoted as follows:

$$\delta\hat{v}_{i,p} = \hat{v}_{i,p,1} - \hat{v}_{i,p,0}$$

$$\delta\Delta\hat{v}_i = \Delta\hat{v}_{i,1} - \Delta\hat{v}_{i,0}$$

$$\delta\hat{\mu}_i = \hat{\mu}_{i,1} - \hat{\mu}_{i,0}$$

The previously estimated standard deviations can be used to estimate standard deviations and CIs for any of the difference statistics denoted by δ. For example, the estimated standard deviation for $\delta\hat{v}_{i,85}$ is calculated as follows:

$$\delta\hat{\sigma}_{v_{i,85}} = \sqrt{\hat{\sigma}^2_{v_{i,85},1} + \hat{\sigma}^2_{v_{i,85},0} + Cov\left((\hat{v}_{i,85})_1, (\hat{v}_{i,85})_0\right)}$$

Travel times, denoted as t_j, between two points are extracted from the data where j is a single bus.

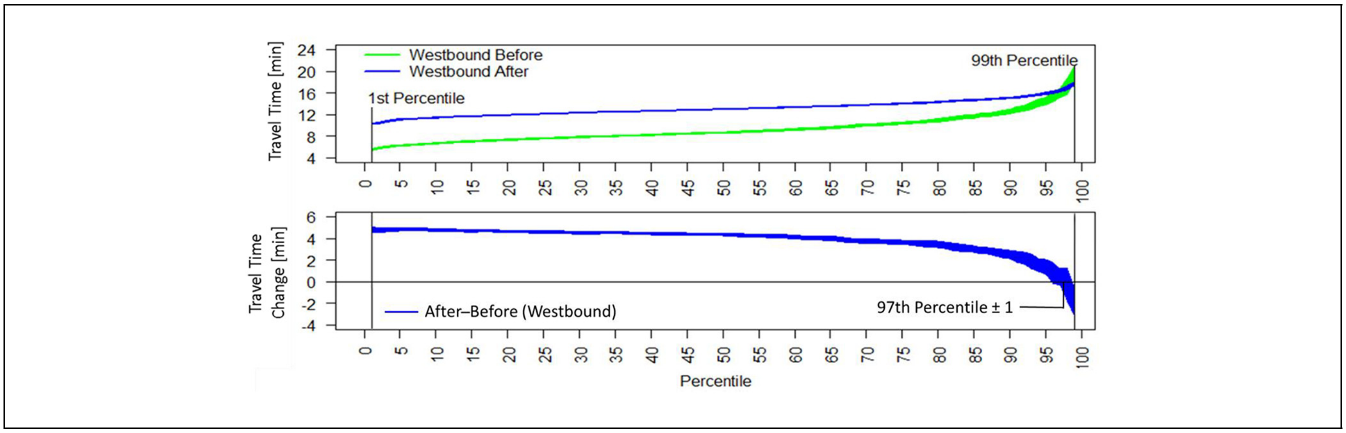

Figure 5. Top: Westbound travel-times. Bottom: travel-time difference (after minus before).

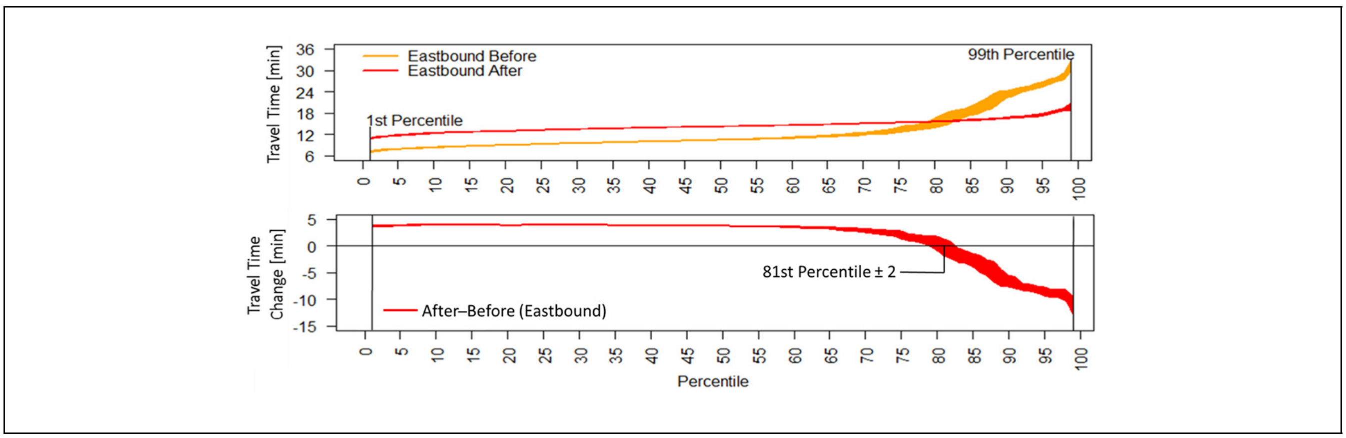

Figure 6. Top: Eastbound travel-times. Bottom: travel-time difference (after minus before).

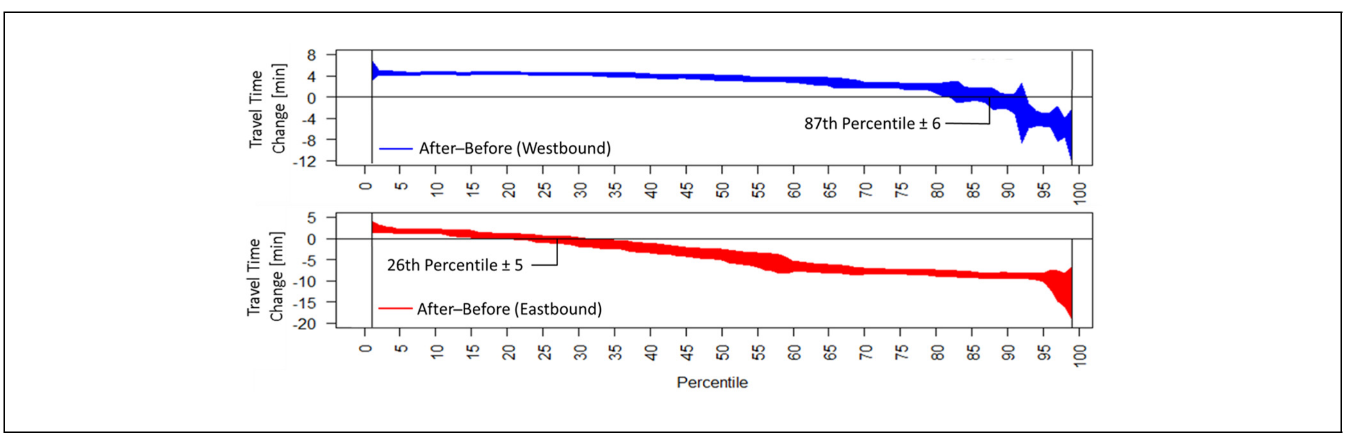

Figure 7. Travel-time differences (after minus before) during the PM peak. Top: westbound. Bottom: eastbound.

Percentiles and CIs are calculated using the same methodology as above.

$\hat{t}_p =$ percentile travel-time, and
$\hat{\sigma}_{tp} =$ standard deviation of percentile travel-time.

Average travel-time, $\bar{t}$, can be found by summing each percentile travel-time as if it were an individual bus then correcting for the number of buses n_{J_i}. On average each percentile travel-time should be seen an equal number of times.

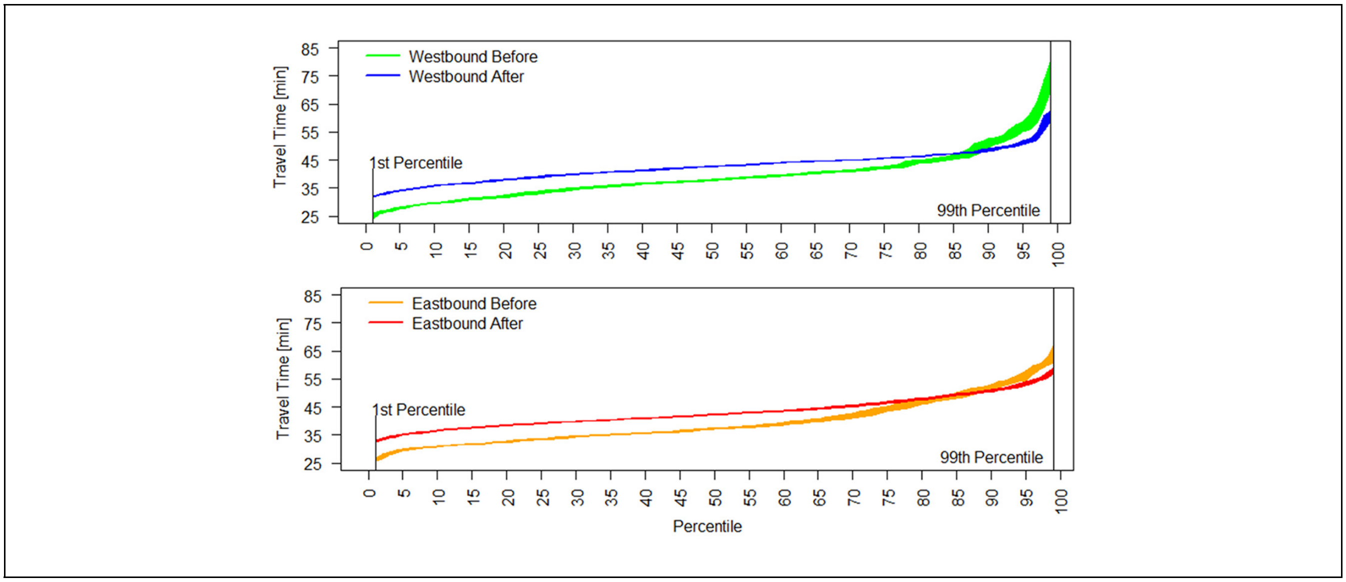

Figure 8. Travel times over 7.2 miles (11.6 km) of Powell for all trips. Top: westbound. Bottom: eastbound.

Table 1. Mean Hourly Travel-Time, Standard Deviation, Passenger Load, and Scheduled Trips per Day

Time	Mean travel-time (min)				Travel-time standard deviation (min)				Mean passenger load				EB trips per day	WB trips per day
	EB		WB		EB		WB		EB		WB			
	bef.	aft.	bef.	aft.	bef.	aft.	bef.	aft.	bef.	aft.	bef.	aft.		
6:00	31.4	36.2	34.2	38.9	2.5	1.4	3.3	2.9	4	2	10	9	3	6
7:00	34.1	40.1	47.8	48.5	2.8	2.7	10.2	5.7	4	4	11	12	3	8
8:00	35.1	40.2	50.5	51.2	2.4	2.4	10.7	7.7	4	4	12	14	5	6
9:00	34.9	40.2	40.9	44.0	3.0	2.5	6.7	3.5	5	4	11	11	4	4
10:00	33.0	40.9	36.4	42.8	19.9	1.8	2.8	3.3	5	5	7	11	4	4
11:00	35.6	42.3	38.2	44.4	2.5	2.3	2.9	4.0	5	6	7	11	4	4
12:00	37.8	44.6	38.6	44.1	2.3	3.6	3.2	2.7	6	8	9	8	4	4
13:00	39.3	44.3	39.0	43.8	2.5	2.3	3.7	3.0	9	7	7	11	4	4
14:00	39.1	45.8	41.0	43.9	2.3	2.8	5.5	3.7	8	11	7	9	5	4
15:00	46.4	49.2	41.8	45.1	7.0	4.4	4.6	4.2	12	12	8	10	6	5
16:00	50.4	51.4	42.0	44.8	5.7	4.5	6.6	2.2	13	12	8	10	8	5
17:00	52.9	50.4	47.4	44.8	6.0	4.2	11.8	3.4	10	14	7	8	9	4
18:00	45.4	45.5	38.3	42.2	7.7	3.9	9.0	3.1	12	12	9	7	5	5
19:00	34.3	41.9	33.4	40.9	14.5	2.9	2.4	2.6	10	10	5	6	4	3
20:00	33.3	40.8	30.8	38.2	2.2	3.8	2.3	2.4	8	8	7	7	4	3

Note: EB = eastbound; WB = westbound; aft. = after; bef. = before.
Travel times are for the same distance covered in Figure 8.

$$\bar{t} = \frac{n_{J_i}}{99}\sum_{p=1}^{99}\hat{t}_p$$

Results

Travel-Time Changes

Travel times in both directions of travel across the Ross Island Bridge—the former river crossing for this route—increased for the vast majority of trips. For westbound travel (Figure 5), it is likely that only a few percent of trips saw a decrease in travel times. For eastbound trips (Figure 6), approximately 20% of trips saw a reduction in travel times. However, although travel times increased for most trips, both directions experienced a large decrease in travel-time variability (i.e., the difference between the 99th and 1st percentile).

The top panels of figures 5 and 6 show the actual travel-times by percentiles with the 95th percentile CI shown. The bottom panel of each figure shows the

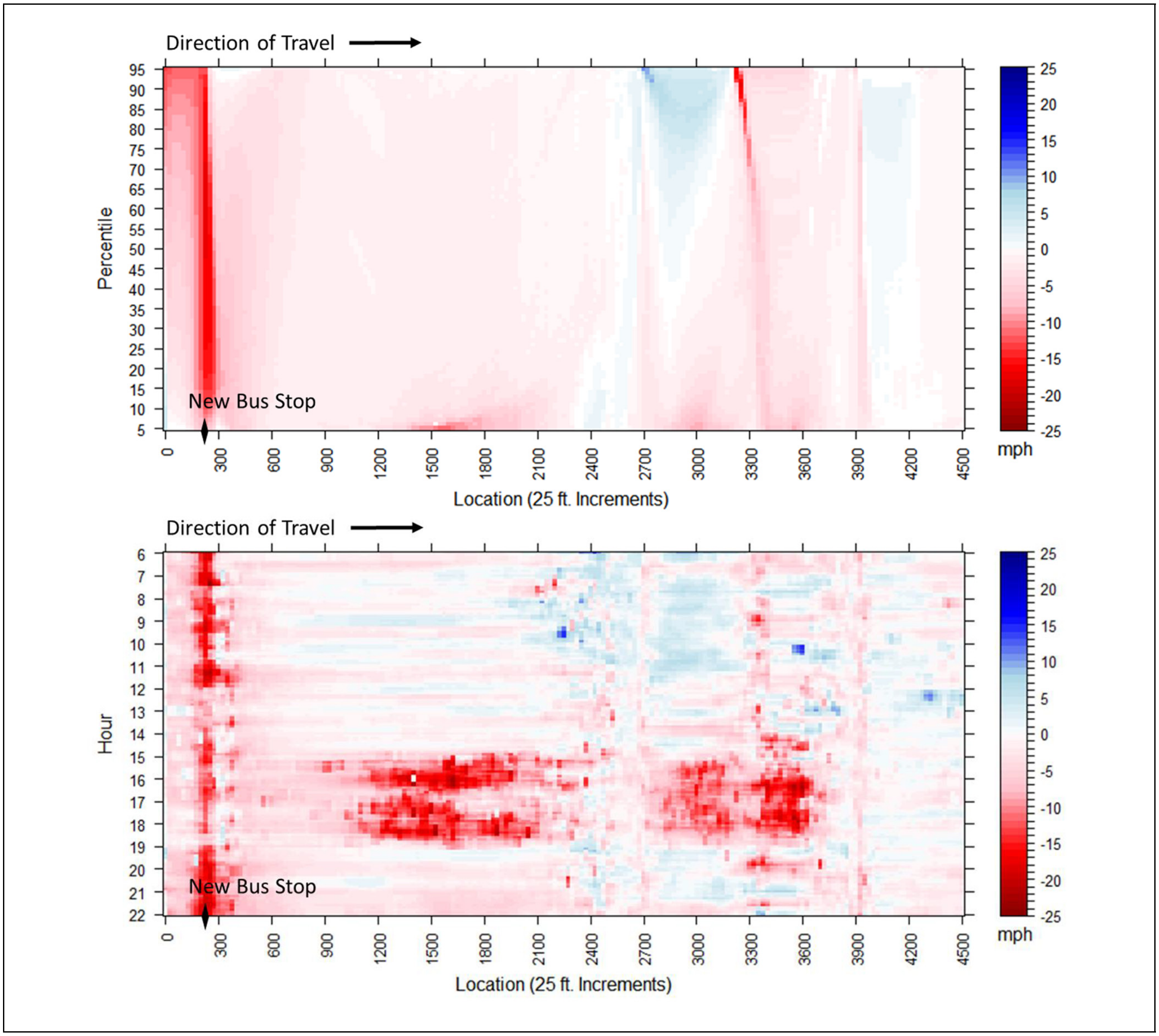

Figure 9. Top: difference in the 5th through 95th percentile travel speeds between before-and-after cases along Powell in the eastbound direction. Bottom: difference in the travel speeds between before-and-after cases along Powell in the eastbound direction by time of day. Each value is created using a 30-min moving average.

estimated difference with positive values indicating longer travel-times between the 1st and 99th percentile. In Figure 5, the travel-time change does not consider the 0.2-mile increase in travel distance for westbound trips. Assuming slow transit speeds of just 15 mph (~24 kph), that distance increase accounts for less than a minute of the total change.

The same type of analysis was conducted for the AM and PM peak periods in both directions. Although, the AM peak showed nearly identical results as the all-day case in both directions, the PM peak saw significant changes in travel times. Figure 7 shows the PM peak travel-time changes (after minus before) for westbound trips (top) and eastbound trips (bottom).

Estimates of travel times were expanded to include an additional 5 mi of Route 9; the resulting 7-mi segment is the most heavily congested part of Powell. As shown in Figure 8, travel times increased for approximately 85% of all trips; however, the range of possible travel times (99th minus 1st percentile) decreased by 23 and 17 min in the westbound and eastbound directions, respectively, despite increases in peak-hour congestion in the Portland metro.

Additionally, as indicated by Table 1, average travel-time became much more consistent by time of day after

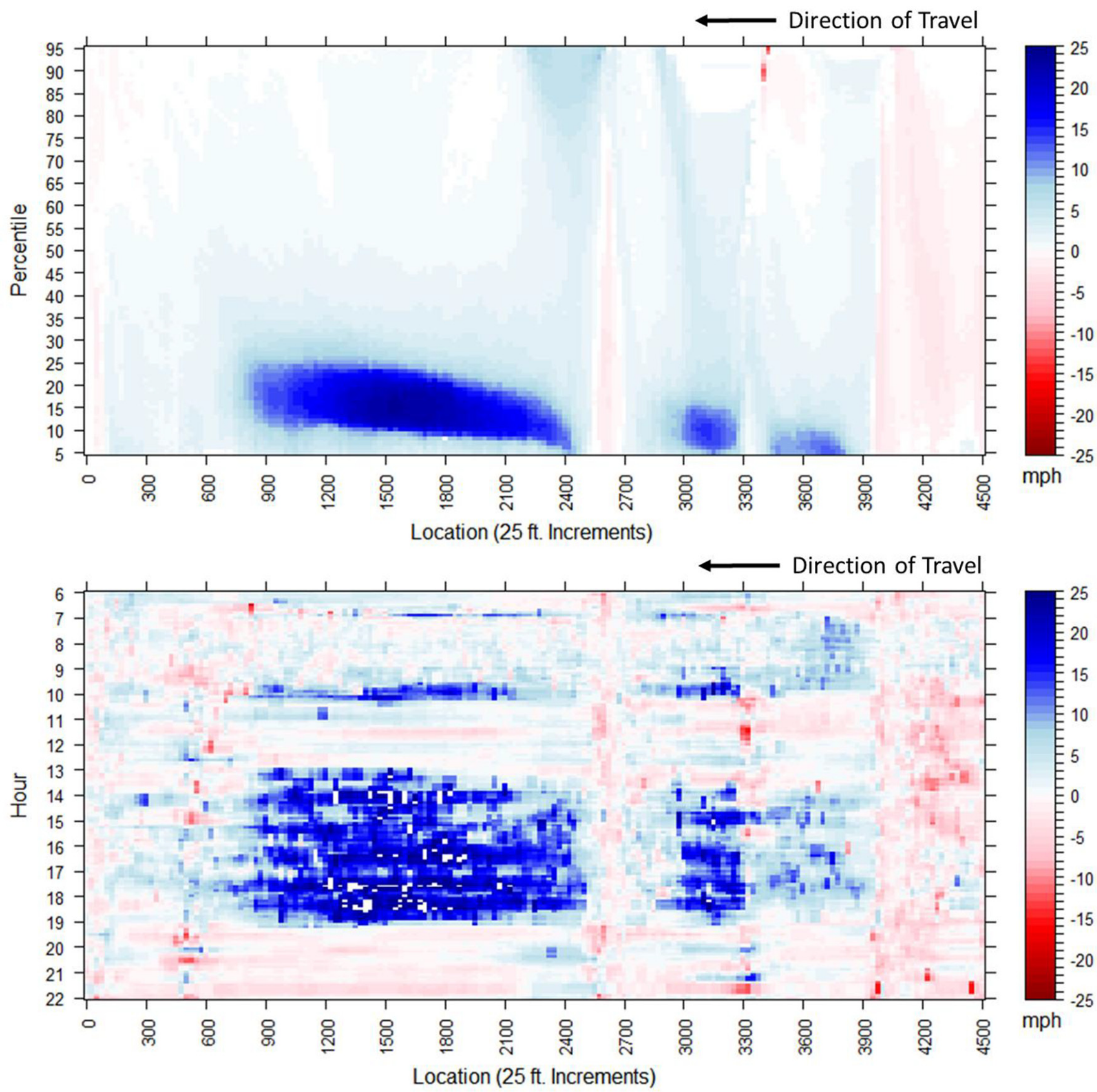

Figure 10. Top: Difference in the 5th through 95th percentile travel speeds between before-and-after cases along Powell in the westbound direction. Bottom: Difference in the travel speeds between before-and-after cases along Powell in the westbound direction by time of day. Each value is created using a 30-minute moving average.

the change. For example, the sharp increase in travel times in eastbound travel at 17:00 is notably reduced after the route change. Passenger loading remains similar.

Eastbound Travel Speeds

The travel speed differences following the changes to Powell indicate substantial changes to bus performance. However, the study area (excluding where route changed) was not significantly altered. The road was repainted without altering the location of lines. The decrease in speed in Figure 9 at $x = 250$ ft ($\sim$76.2 m) is accounted for by the addition of a new bus stop. Prior to the change in the route, that bus stop was a nearside stop approximately 50 ft ($\sim$15 m) before the start of the analysis area. The before and after routes do not overlap. As such, the previous bus stop and the new left turn on the route were excluded. By percentile, much of eastbound travel appears to have decreased in speed. By time of day, the majority of the decreased speed is seen to be in the peak period.

Westbound Travel Speeds

For westbound travel, travel speeds increased significantly for the 10th through 25th percentiles. This

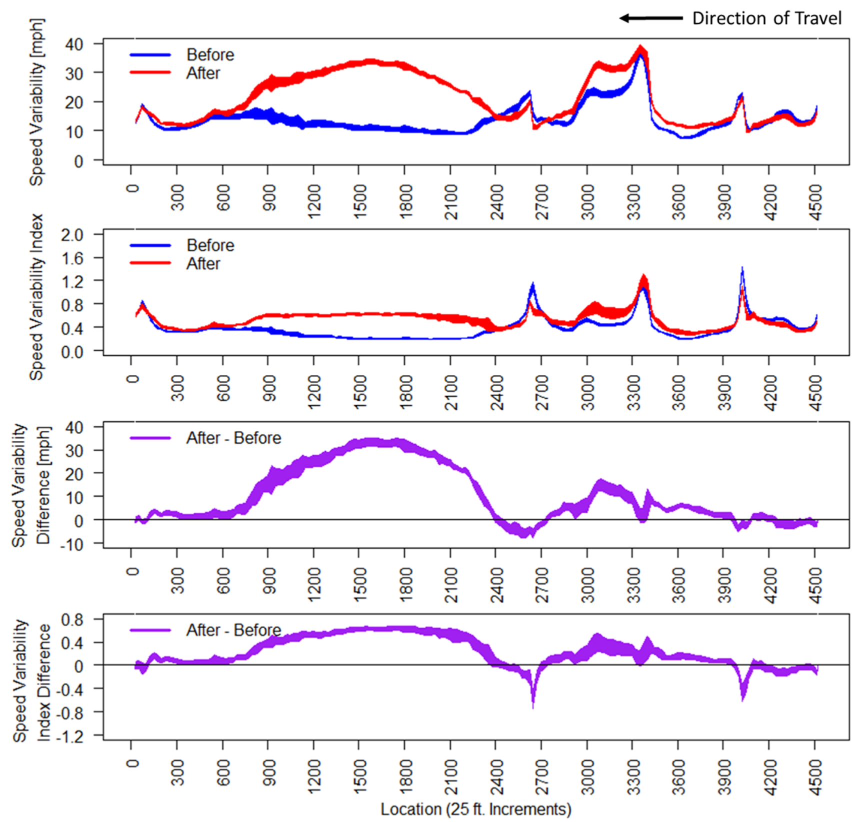

Figure 11. All graphs: westbound direction on Powell. Thickness of line is the 95th percentile confidence interval. Top: speed variability (85th minus 15th percentile travel speed) in miles per hour. Upper middle: speed variability index (ratio between the speed variability and 50th percentile travel speeds). Lower middle: difference between speed variability. Bottom: difference between speed variability index.

decreased travel-time is concentrated during the evening commute. Traffic patterns suggest that, typically, vehicles are attempting to leave the city center. The time-of-day plot in Figure 10 shows that there is less congestion heading into the city after the route change than there was before.

This major change in traffic patterns is supported by the plots of speed percentile difference and the speed variability index in Figure 11, which shows different traffic patterns before and after the change, as well as a large non-zero difference between them. In the eastbound direction, the differences in speed variability and the speed variability index show near zero and statistically insignificant changes.

Conclusion

The methodologies outlined in this paper provide a means to quantify differences in transit performance on roadway segments from before and after a change to that roadway. HR GPS data can provide detailed information between stops and highlight areas and times-of-day in which speeds or travel times differ and can be applied to different types of roadway reconfigurations. Furthermore, the use of percentile CIs can provide insights into how travel-time variability changes at different locations and travel speeds.

TriMet's claim that travel times would decrease is not clear from the results of this data. For the majority of trips, travel times actually increased for Route 9. One contributing factor to the increased travel-times may be the 25-mph (~40-kph) speed limit for buses and trains (*3*). This limit is a product of line-of-sight requirements that are limited by the grade of the bridge, which, to provide enough clearance for ships, is just under 5% for the majority of its length (*25*). Another factor may be the wait time at traffic signals around the new bridge. These signals give priority to light rail and force buses to wait to keep space between the two travel modes. In terms of efficiency, travel appears significantly more predictable due to the dramatic difference in travel-time variability during the peak period. This predictability may reduce the need for added and unscheduled buses during peak congestion, which may reduce long-term costs.

Acknowledgments

The authors thank Steve Callas and Miles J. Crumley of TriMet for providing the data sets used in this analysis and for their support in understanding the intricacies of how the data are structured. The authors also acknowledge the support of National Institute for Transportation and Communities transportation center for funding this research effort.

Author Contributions

The authors confirm contribution to the paper as follows: study conception and design: Glick, Figliozzi; data collection: Tri-County Metropolitan District of Oregon (TriMet); analysis and interpretation of results: Glick, Figliozzi; draft manuscript preparation: Glick, Figliozzi.

References

1. Levinson, H. S. Analyzing Transit Travel Time Performance. *Transportation Research Record: Journal of the Transportation Research Board*, 1983. 915: 1–6.
2. Portland Bureau of Transportation. *Tilikum Crossing: Bridge of the People*. The City of Portland [Online]. 2015. Accessed: May 2017. https://www.portlandoregon.gov/transportation/68548.
3. TriMet. *Tilikum Crossing Bridge of the People*. TriMet [Online]. 2015. Accessed: May 2017. https://trimet.org/tilikum/.
4. Persuad, B., and C. Lyon. Empirical Bayes Before–After Safety Studies: Lessons Learned from Two Decades of Experience and Future Directions. *Accident Analysis & Prevention*, Vol. 39, No. 3, 2007, pp. 546–555.
5. Hauer, E. *Observational Before-After Studies in Road Safety*. Elsevier Sciences Ltd., Oxford, 1997.
6. Hauer, E., and B. Persaud. Common Bias in Before-and-Bfter Accident Comparisons and Its Elimination. *Transportation Research Record: Journal of the Transportation Research Board*, 1983. 905: 164–174.
7. Farmer, C. M., A. K. Lund, R. E. Trempel, and E. R. Braver. Fatal Crashes of Passenger Vehicles Before and After Adding Antilock Braking Aystems. *Accident Analysis & Prevention*, Vol. 29, No. 6, 1997, pp. 745–757.
8. Huang, H. F., and M. J. Cynecki. Effects of Traffic Calming Measures on Pedestrian and Motorist Behavior. *Transportation Research Record: Journal of the Transportation Research Board*, 2000. 1705: 26–31.
9. Ringner, B. Law of the Unconscious Statistician. *Unpublished Note*, 2009.
10. Glick, T. B., and M. A. Figliozzi. Traffic and Transit Travel Time Reliability Indexes and Confidence Intervals. *Transportation Research Record: Journal of the Transportation Research Board*, 2017. 2649: 28–41.
11. Ayvalik, C. K., and Jotin Khisty, C. Heuristic Analysis of Impacts of Commuter Rail Station Consolidation on Pedestrian Access. *Tranportation Research Record: Journal of the Transportation Research Board*, 2002. 1793: 47–54
12. Kim, K. "Metro Travel Forcasting 2008 Trip-Based Demand Model Methology Report" Planning Department - Transportation Research and Modeling Services, 2008.
13. Hall, R., and N. Vyas. Buses as a Traffic Probe: Demonstration Project. *Transportation Research Record: Journal of the Transportation Research Board*, 2000. 1731: 96–103.
14. Cathey, F., and D. Dailey. Transit Vehicles as Traffic Probe Sensors. *Transportation Research Record: Journal of the Transportation Research Board*, 2002. 1804: 23–30.
15. Bertini, R., and S. Tantiyanugulchai. Transit Buses as Traffic Probes: Use of Geolocation Data for Empirical Evaluation. *Transportation Research Record: Journal of the Transportation Research Board*, 2004. 1870: 35–45.
16. Berkow, M., M. Wolfe, C. Monsere, and R. Bertini. Using Signal System Data and Buses as Probe Vehicles to Define the Congested Regime on Arterials. Presented at 87th Annual Meeting of the Transportation Research Board, Washington D.C., 2008.
17. Skabardonis, A., and N. Geroliminis. Real-time Estimation of Travel Times on Signalized Arterials. *Proc. 16th International Symposium on Transporation and Traffic Theory*, College Park, MD, 2005, pp. 387–406.
18. Bertini, R. L., and A. M. El-Geneidy. Generating Transit Performance Measures with Archived Data. *Transportation Research Record: Journal of the Transportation Research Board*, 2003. 1841: 109–119.
19. Chakroborty, P., and S. Kikuchi. Using Bus Travel Time Data to Estimate Travel Times on Urban Corridors. *Transportation Research Record: Journal of the Transportation Research Board*, 2004. 1870: 18–25.
20. Mazloumi, E., G. Currie, and G. Rose. Using GPS Data to Gain Insight into Public Transport Travel Time Variability. *Journal of Transportation Engineering*, Vol. 136, No. 7, 2010, pp. 623–631.
21. Crumley, M. Interviewee, Operational TriMet Questions [Interview]. 2017.
22. *Portland Region 2016 Traffic Performance Report*. Oregon Department of Transportation, 2016.
23. Brown, M. B., and R. A. Wolfe. Estimation of the Variance of Percentile Estimates. *Computational Statistics & Data Analysis*, Vol. 1, 1983, pp. 167–174.
24. Taylor, J. R. *An Introduction to Error Analysis The Study of Uncertainties in Physical Measurements*. University Science Books, Sausalito, Calif., 1997.
25. Anderston, M. *Tilikum Crossing: A Few Words of Advice for Folks Working to Conquer Hills*. Bike Portland [Online], 2015. Accessed. May 2017. https://bikeportland.org/tag/tilikum-crossing.

The Public Transportation Group (AP000) peer-reviewed this paper (18-06530).

Any errors or omissions are the sole responsibility of the authors.